Quantitative Measurement of Cytosolic and Nuclear Penetration of Oligonucleotide Therapeutics

Kirsten Deprey, Nefeli Batistatou, Marjoke F. Debets, Jack Godfrey, Kirstin B. VanderWall,
Rebecca R. Miles, Livia Shehaj, Jiaxing Guo, Amy Andreucci, Pachamuthu Kandasamy, Genliang Lu,
Mamoru Shimizu, Chandra Vargeese, and Joshua A. Kritzer*

ACCESS | Metrics & More | Article Recommendations | Supporting Information

ABSTRACT: A major obstacle in the development of effective oligonucleotide therapeutics is a lack of understanding about their cytosolic and nuclear penetration. To address this problem, we have applied the chloroalkane penetration assay (CAPA) to oligonucleotide therapeutics. CAPA was used to quantitate cytosolic delivery of antisense oligonucleotides (ASOs) and siRNAs and to explore the effects of a wide variety of commonly used chemical modifications and their patterning. We evaluated potential artifacts by exploring the effects of serum, comparing activity data and CAPA data, and assessing the impact of the chloroalkane tag and its linker chemistry. We also used viral transduction to expand CAPA to the nuclear compartment in epithelial and neuronal cell lines. Using this enhanced method, we measured a 48-h time course of nuclear penetration for a panel of chemically diverse modified RNAs. Moving forward, CAPA will be a useful tool for deconvoluting the complex processes of endosomal uptake, escape into the cytosol, and subcellular trafficking of oligonucleotide therapeutics in therapeutically relevant cell types.
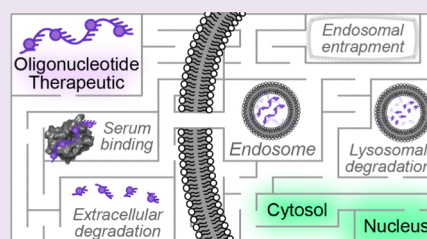
INTRODUCTION

Oligonucleotide therapeutics are a particularly promising strategy to treat currently intractable diseases including neurodegenerative diseases, autoimmune disorders, cancers, and rare genetic diseases.[1] However, oligonucleotide therapeutics can have poor tissue distribution and poor cell penetration. This leads drug developers to pursue high dosing levels, which can lead to increased toxicity.[2] Thus, a critical obstacle for oligonucleotide therapeutics is a relative lack of understanding of cell uptake, cytosolic localization, and intracellular trafficking.[3−5]

Internalization pathways for oligonucleotide therapeutics are often separated into "nonproductive" pathways, such as endosomal entrapment, and "productive" pathways that allow access to the nuclear and/or cytosolic target.[4] Some chemically modified oligonucleotides can access the cytosol without additional delivery vectors, through a process referred to as gymnosis or gymnotic uptake.[6] During gymnotic uptake, oligonucleotide therapeutics are primarily taken up through endocytosis or macropinocytosis. A large proportion of this material becomes trapped in endosomes or trafficked to the lysosome, but a small amount can escape and access the cytosol and/or nucleus. A major barrier to understanding productive gymnotic uptake, and thus designing oligonucleotide therapeutics with improved cytosolic penetration, is the qualitative nature of most cell penetration assays. Further, many commonly used assays for cell penetration cannot measure cytosolic and nuclear penetration distinctly from the endosomally trapped material.[7] Recent work has also high-lighted the pitfalls of using fluorescently labeled oligonucleotides to measure cytosolic penetration, including artifacts due to degradation, fixation methods, and other parameters.[7,8]

We recently developed the chloroalkane penetration assay (CAPA) to quantitatively measure the cytosolic and nuclear localization of chloroalkane-tagged peptides.[9,10] In this work, we report the first application of CAPA to synthetic oligonucleotides. Further, we report the adaptation of CAPA for use in multiple cell lines using adeno-associated virus (AAV) to introduce the required compartment-localized HaloTag fusion. The newfound ability to perform CAPA in AAV-transduced cells will be highly valuable in the design of oligonucleotide therapeutics that are maximally penetrant in specific tissue types.

RESULTS AND DISCUSSION

Application of CAPA to Clinically Relevant Oligonucleotides. The chloroalkane penetration assay (CAPA) measures the cytosolic localization of a chloroalkane-tagged compound.[9] The cells used for CAPA express a modified haloalkane dehalogenase, called HaloTag, exclusively in the cytosol.[11] HaloTag reacts irreversibly with a small chloroalkane
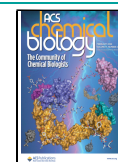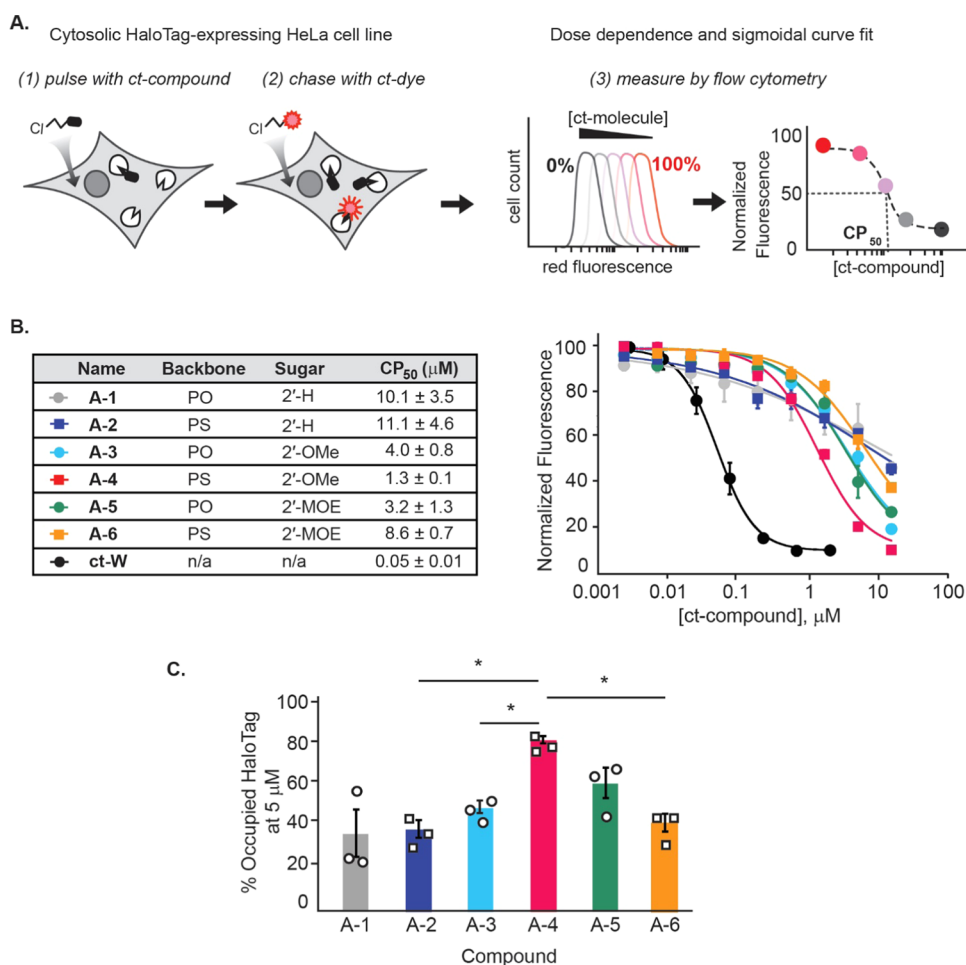
Figure 1. Application of the Chloroalkane Penetration Assay (CAPA) to ASOs. (A) Schematic of CAPA. HeLa cells expressing cytosolic HaloTag are pulsed with chloroalkane-tagged RNA and chased with a chloroalkane-tagged dye. Red fluorescence, measured by flow cytometry, is inversely proportional to the cytosolic concentration of ct-RNA. Mean red fluorescence values for each sample are normalized to background fluorescence (0%) and fluorescence from cells treated only with chloroalkane-dye (100%), dose dependence of the red fluorescence is plotted, and sigmoidal curves are fit to determine half-maximal intensity values, which we refer to as CP_{50}.[9,10] (B) Dose-dependent CAPA curves and CP_{50} values for the small-molecule control ct-W and six compounds with nusinersen-like sequence A (SI Table 1) with various combinations of commonly used backbone and sugar modifications. Phosphodiester backbones are denoted PO, phosphorothioate backbones are denoted PS, deoxyribose sugars are denoted 2′-H, sugars with 2′-O-methyl modifications are denoted 2′-OMe, and sugars with 2′-O-methoxyethyl modifications are denoted 2′-MOE. (C) Percent occupied HaloTag was calculated from the CAPA signal of each compound. Asterisks indicate p values <0.001 using a two-tailed t-test. Error bars show standard error from three independent trials, and CP_{50} values are reported as average and standard error from three independent curve fits to three independent trials.

group.[12] In CAPA, HaloTag-expressing cells are pulsed with a chloroalkane-tagged compound (ct-compound), and if the molecule is able to access the cytosol, it blocks HaloTag active sites. Cells are then chased with a cell-permeable chloroalkane-tagged dye (ct-dye), which reacts with all open HaloTag active sites. Fluorescence is measured by flow cytometry and plotted as a function of ct-compound concentration used in the pulse step (Figure 1A). Mean fluorescence values from flow cytometry are fit to a sigmoidal dose–response curve, and the concentration of the ct-compound at which 50% of the HaloTag is blocked is calculated from the curve fit. We use this value, referred to as the CP_{50}, to compare the extent of cytosolic localization among ct-compounds.[9,10] Structures of ct-compounds and sequences of ct-RNAs used in this study are included in SI Figure 1 and SI Table 1.

We first benchmarked CAPA with a series of antisense oligonucleotides (ASOs) that had a base sequence similar to nusinersen, which was approved by the US FDA in 2016 for

the treatment of spinal muscular atrophy.[13] The nusinersen-like sequence was prepared with either phosphodiester (PO) or phosphorothioate (PS) backbone and either 2′-H (DNA), 2′-O-methyl (2′-OMe), or 2′-O-methoxyethyl (2′-MOE) on the ribose sugar (compounds A-1 through A-6). These oligonucleotides were labeled on the 5′ end with a chloroalkane tag and used in CAPA experiments in serum-free medium with 4 h of incubation. ct-ASOs composed of deoxyribonucleotides with PO or PS backbones, A-1 and A-2, were the least cytosolically penetrant; however, the broad slopes of their concentration curves compared to all other ASOs tested (see below) may be indicative of unusual degradation, aggregation, or other behavior.[8,10] The ct-ASO with the PS backbone and 2′-OMe modifications, A-4, was the most cytosolically penetrant, with a CP_{50} of 1.3 μM. Surprisingly, the oligonucleotide with a PS backbone and 2′-MOE modifications, A-6, had comparatively poor cell penetration at 4 h, with a CP_{50} of 8.6 μM (Figure 1B). At 5
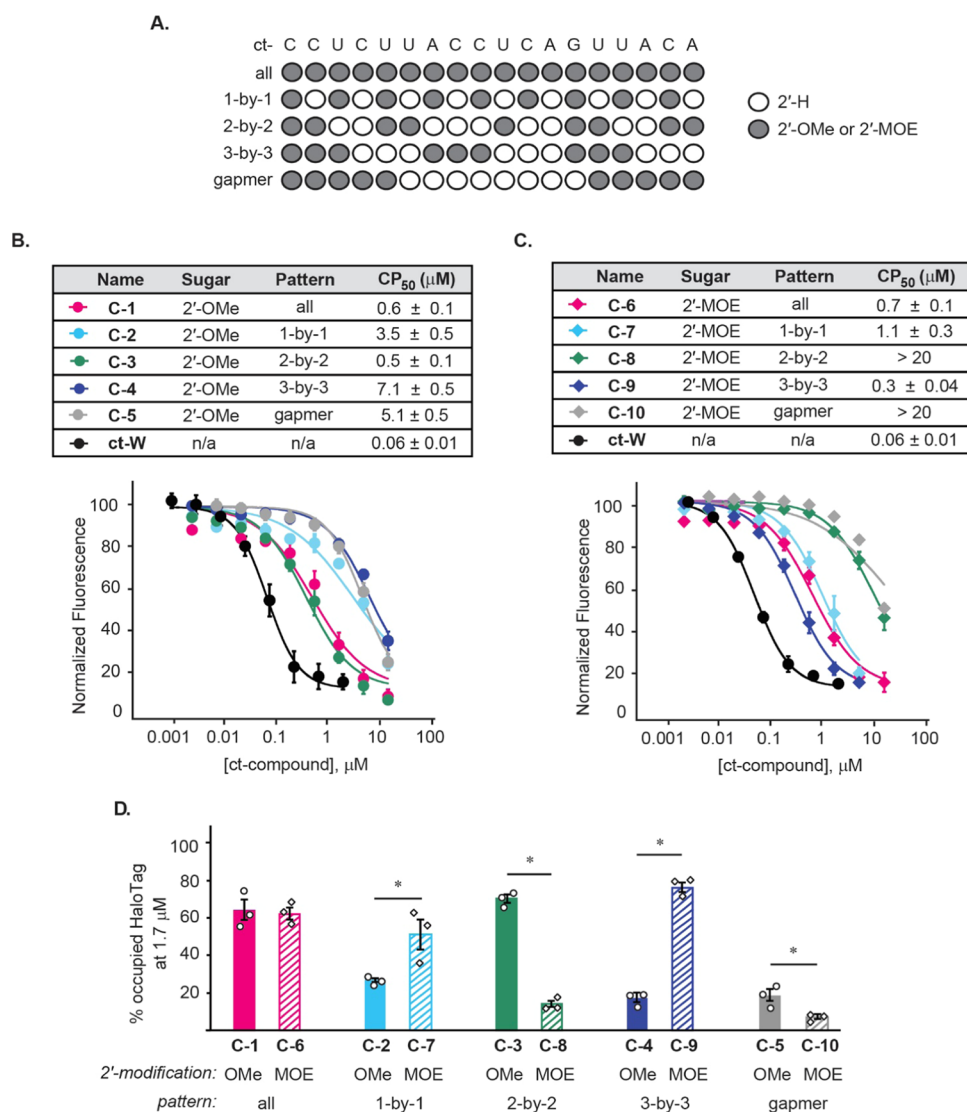
Figure 2. Effects of 2′ modification patterning on cytosolic localization. (A) Schematic of patterns tested. Gray circles represent sugars that are modified at the 2′ position and white circles represent deoxyribose sugars; backbones are entirely modified with phosphorothioates. The sequence is designed to be compatible with splice correction in a cell-based luciferase reporter assay (see SI, Figure 4). (B) Dose-dependent CAPA curves and CP_{50} values for oligonucleotides with 2′-O-methyl (2′-OMe) modification patterns. (C) Dose-dependent CAPA curves and CP_{50} values for oligonucleotides with 2′-O-methoxyethyl (2′-MOE) modification patterns. (D) Percent occupied HaloTag was calculated from the CAPA signal of each compound. Cells were incubated with the indicated concentration of ct-RNA for 4 h in serum-free media. Asterisks indicate p values <0.05 using a two-tailed t-test. Error bars show standard error from three independent trials, and CP_{50} values are reported as average and standard error from three independent curve fits to three independent trials.

μM, the ct-ASO with a PS-2′-OMe backbone, **A-4**, had significantly enhanced cytosolic localization compared to analogues with PO, DNA, or 2′-MOE backbones (Figure 1C).

We performed similar experiments on oligonucleotides with a second clinically relevant sequence, that of alicaforsen, which targets the mRNA of intercellular adhesion molecule-1.[14] The alicaforsen-like panel (compounds **B-1** through **B-4**) showed similar results to the nusinersen-like panel (SI, Figure 2 and SI, Table 2). Overall, CAPA recapitulated the expected result that ASOs with more highly modified backbones are generally more cytosolically penetrant than unmodified ASOs.

While the effects of backbone modifications on cellular internalization are generally assumed to be independent of the oligonucleotide sequence,[15] we observed different trends in cytosolic penetration for the nusinersen-like sequence and the alicaforsen-like sequence with respect to different backbone

modifications (SI Figure 3). These data imply that cytosolic penetration is affected by cooperative contributions from sequence, length, and backbone modifications.

Effects of Modification Patterning for Splice-Correcting ASOs. Cellular activity is a complex measurement that integrates many factors including intrinsic potency, cell uptake, vesicular trafficking, endosomal escape, degradation, and off-target binding. We next sought to compare cellular activity data to CAPA data, which is a direct measurement of cytosolic penetration. For this purpose, we used a third sequence that was compatible with a luciferase-based reporter assay for splice-switching at the β-globin intron, described previously (SI Figure 4A).[16]

Patterning of the backbone and sugar modifications is frequently used to optimize the pharmacological properties of oligonucleotide therapeutics.[17,18] The effects of different
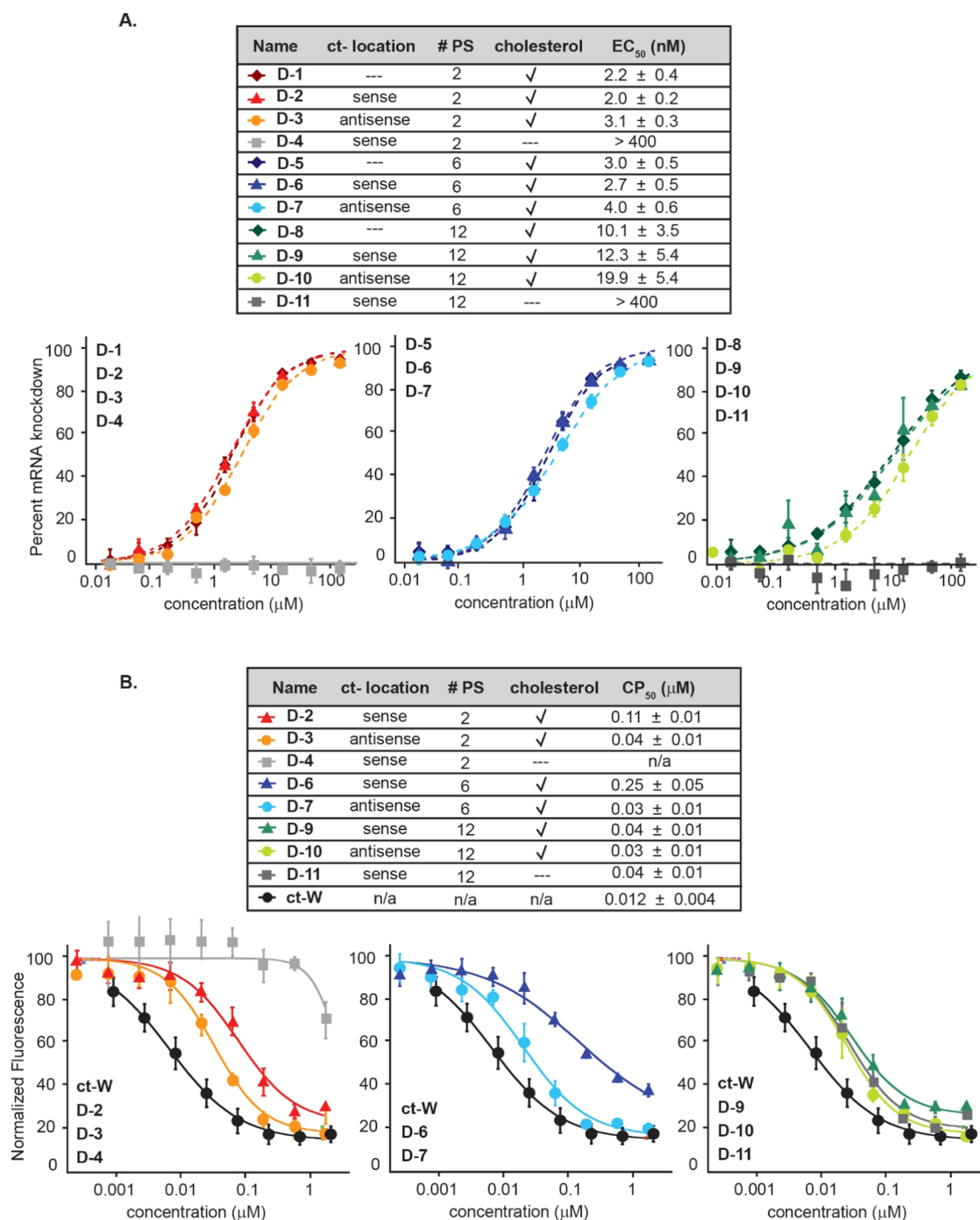
A.

	Name	ct- location	# PS	cholesterol	EC_{50} (nM)
◆	D-1	---	2	✓	2.2 ± 0.4
▲	D-2	sense	2	✓	2.0 ± 0.2
●	D-3	antisense	2	✓	3.1 ± 0.3
■	D-4	sense	2	---	> 400
◆	D-5	---	6	✓	3.0 ± 0.5
▲	D-6	sense	6	✓	2.7 ± 0.5
●	D-7	antisense	6	✓	4.0 ± 0.6
◆	D-8	---	12	✓	10.1 ± 3.5
▲	D-9	sense	12	✓	12.3 ± 5.4
●	D-10	antisense	12	✓	19.9 ± 5.4
■	D-11	sense	12	---	> 400

B.

	Name	ct- location	# PS	cholesterol	CP_{50} (μM)
▲	D-2	sense	2	✓	0.11 ± 0.01
●	D-3	antisense	2	✓	0.04 ± 0.01
■	D-4	sense	2	---	n/a
▲	D-6	sense	6	✓	0.25 ± 0.05
●	D-7	antisense	6	✓	0.03 ± 0.01
▲	D-9	sense	12	✓	0.04 ± 0.01
●	D-10	antisense	12	✓	0.03 ± 0.01
■	D-11	sense	12	---	0.04 ± 0.01
●	ct-W	n/a	n/a	n/a	0.012 ± 0.004

Figure 3. Application of CAPA to siRNAs. (A) Dose-dependent activity curves and EC_{50} values for HPRT mRNA knockdown, grouped by the total number of phosphorothioate modifications. (B) Dose-dependent CAPA curves and CP_{50} values for small-molecule control ct-W and all siRNAs, grouped by the total number of phosphorothioate modifications. Cells were incubated with the indicated concentration of ct-siRNA for 48 h in serum-free media. Error bars show standard error from three independent trials, and CP_{50} values are reported as average and standard error from three independent curve fits to three independent trials.

patterns are often measured using activity assays, but to our knowledge, there have not yet been reports that directly compare the *cytosolic localization* of ASOs with different modification patterns. We prepared phosphorothioate RNAs with the same sequence but with five different patterns of 2′ modifications (**C-1** through **C-6**, Figure 2A). In experiments using either lipofectamine-facilitated delivery or gymnotic delivery, the 1-by-1, 2-by-2, and 3-by-3 alternating patterns of 2′ modifications had less activity than all-modified ASOs (SI,

Figure 4B,C). Though alternating patterns reduced activity, we applied CAPA to examine if different patterns would affect the degree of cytosolic localization. The all-modified compounds **C-1** and **C-6** (PS-2′-OMe and PS-2′-MOE modifications, respectively) showed comparable activity in CAPA and in the reporter assay (Figure 2B,C, and SI, Figure 4B). For the patterned compounds, the CAPA-derived CP_{50} values had a fairly wide range. Unexpectedly, compound **C-3** (2-by-2 alternating pattern of 2′-OMe modifications) was 7- to 15-

fold more penetrant than the other patterns and similarly penetrant as the all-modified analogue **C-1** (Figure 2B). By contrast, for the PS-2′-MOE modification, the 2-by-2 alternating pattern, compound **C-8**, was one of the least penetrant. Instead, the 3-by-3 alternating pattern, compound **C-9**, was among the most cytosolically penetrant, even when compared to the all-modified analogue **C-6** (Figure 2C). These differences are also clear when comparing different patterns and modifications at a single concentration point (Figure 2D). Overall, these data demonstrate that the nature of each modification, the number of modifications, and their relative locations within the ASO work synergistically when it comes to cytosolic localization. While CAPA alone does not explain all trends observed in activity assays, these data emphasize the utility of CAPA as a tool to isolate cytosolic penetration from other factors affecting activity when assessing ASOs with different chemical modifications and patterns.

Effects of PS Content for Cholesterol-Conjugated siRNAs. We next aimed to use CAPA to compare cytosolic penetration to knockdown activity for a series of chemically modified siRNAs. The siRNAs were labeled with the chloroalkane tag at the 5′ end of the sense strand or the 3′ end of the antisense strand, and they were also labeled with cholesterol at the 3′ position of the sense strand to promote internalization.[19] Four siRNAs were prepared with two phosphorothioate (2PS) modifications, three were prepared with 6PS modifications, and four were prepared with 12PS modifications. Within each group, the presence of the cholesterol tag and the presence and location of the chloroalkane tag were varied to distinguish the effects of each tag on cytosolic penetration, activity, and RISC loading. These siRNAs (compounds **D-1** through **D-11**, Table S1) were targeted to hypoxanthine-guanine phosphoribosyltransferase (HPRT), a common housekeeping gene abundant in HeLa cells that has been used previously as a knockdown target.[20]

First, we measured the knockdown activity of the siRNA series after 48 h of gymnotic uptake. EC_{50} values for HPRT knockdown were not affected by either the presence or the location of the chloroalkane tag but removing the cholesterol abolished activity (Figure 3A). Almost all compounds with 2PS modifications and 6PS modifications had roughly similar knockdown activities, while the compounds with 12PS modifications had 4- to 6-fold lower activity (Figure 3A). Similar trends for activity were observed after a 72 h treatment (SI, Figure 5). When transfected into HeLa cells to bypass gymnotic uptake, the 12PS series also had poorer EC_{50} values than their 2PS and 6PS counterparts (SI, Figure 6), implying that the 12PS siRNAs have poorer intrinsic activity. All compounds had similar duplex stabilities, with T_m values ranging from 67.0 to 70.5 °C (SI, Figure 7). We also measured the extent of RISC loading for each compound and observed no statistically significant changes (SI, Figure 8). Altogether, these measurements provided context to compare the cell penetration of these functional siRNAs.

Next, we applied the siRNAs to CAPA experiments. Surprisingly, the extent of PS modification did not greatly affect apparent cytosolic penetration (Figure 3B), but the location of the chloroalkane tag did for the siRNAs with 2PS modifications (compounds **D-2** and **D-3**) and 6PS modifications (compounds **D-6** and **D-7**). This trend was not observed for the siRNAs with 12PS modifications (compounds **D-9** and **D-10**) perhaps because it is already relatively nonpolar. The

siRNAs with 12PS modifications also had similar CAPA signals with or without cholesterol, while those with 2PS modifications demonstrated substantially improved cytosolic penetration when conjugated to cholesterol. In fact, the 2PS siRNA without cholesterol, compound **D-4**, barely had any CAPA signal at all, even after 48 h (Figure 3B). Thus, the CAPA data suggest that cell penetration of the siRNAs with 12PS modifications was relatively insensitive to the location and identity of hydrophobic tags, but cell penetration of siRNAs with more polar backbones were affected by the attachment of cholesterol groups. Overall, we did not observe a direct correlation between cytosolic penetration and mRNA knockdown for these relatively potent siRNAs (SI, Figure 9), implying that, for these siRNAs, cell penetration is not the sole limiting factor for activity.

Extension of CAPA Using AAV Transduction. CAPA using stably transfected HeLa cells (HGM cells)[11] detects the material that has accessed the cytosol, but splice-switching ASOs and some other oligonucleotide therapeutics exert their actions in the nucleus. To make better comparisons between CAPA data and activity data, we sought a CAPA cell line that could quantitate the material that accessed the nucleus. In a previous report, we used a stable cell line expressing nuclear-localized HaloTag.[9] However, it proved challenging to maintain high, homogenous HaloTag expression levels in this cell line. Thus, we decided to use AAV transduction to introduce a nuclear-localized HaloTag fusion protein into human cells in culture.

We designed AAV-compatible plasmids containing two HaloTag fusion constructs, HaloTag-GFP-mito for a cytosolically oriented HaloTag (SI, Figures 10−11) and Histone2B-GFP-HaloTag for a nuclear-oriented HaloTag (see the Methods section, and SI, Figures 12 and 13). These plasmids were packaged into AAV2 vectors, which were then used to transduce HeLa cells. The expression levels of transduced cells were comparable to the stable HGM cell line but with somewhat broader distributions (SI, Figure 14). To judge CAPA performance in AAV-transduced HeLa cells, we used three positive controls that were tested extensively in previous reports, ct-W, ct-Tat, and ct-Arg9.[9,10] AAV-transduced HeLa cells with either construct produced CP_{50} values for these three compounds that were identical to results with the stable HGM cell line at 24 h or at 48 h after transduction (SI, Figure 15, SI, Tables 5−7). These data support the ability to use AAV transduction, rather than stable cell lines, to produce reliable CAPA data. We note that this procedure adds only 24−48 h and minimal additional processing steps to the overall CAPA protocol.[10]

Measuring Nuclear Penetration and Effects of Serum Using CAPA with AAV-Transduced HeLa Cells. Most ASOs demonstrate activity only after nuclear penetration.[4] Thus, we sought to verify whether the trends observed with cytosolic CAPA were an accurate reflection of nuclear penetration. We selected a panel of diverse RNAs (compounds **A-6**, **C-11**, **D-2**, and **E-5**) and compared their apparent cytosolic and nuclear penetration in HeLa cells (SI, Figure 16A). The CP_{50} values for all compounds were comparable for the stable HGM cell line and the AAV-H2GH-transduced cell line (SI, Figure 16B,C and SI, Table 8). This observation matches a previous report demonstrating comparable cytosolic and nuclear penetration of chloroalkane-labeled peptides,[9] and it matches prior work which implies that cytosol-to-nucleus

A.

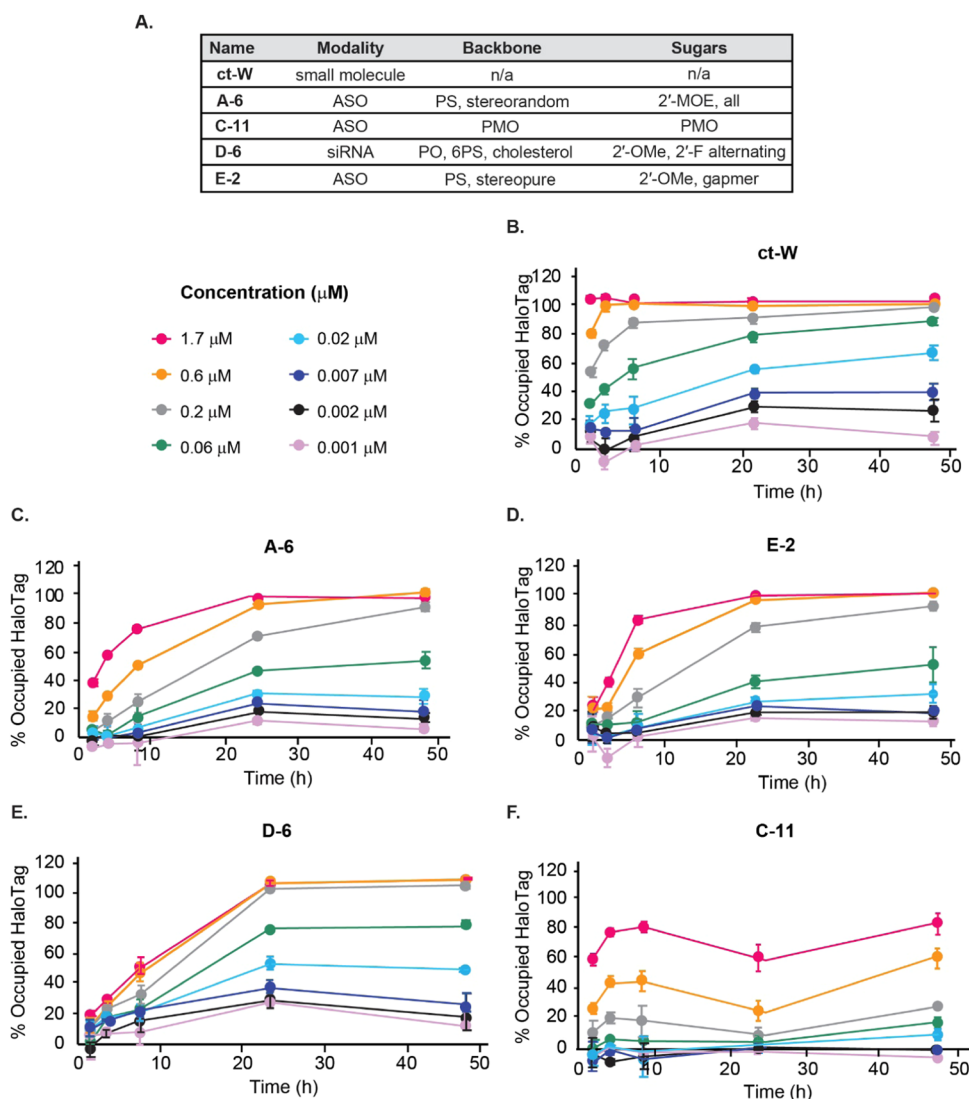| Name	Modality	Backbone	Sugars
ct-W	small molecule	n/a	n/a
A-6	ASO	PS, stereorandom	2'-MOE, all
C-11	ASO	PMO	PMO
D-6	siRNA	PO, 6PS, cholesterol	2'-OMe, 2'-F alternating
E-2	ASO	PS, stereopure	2'-OMe, gapmer

Figure 4. Time course of nuclear penetration for a panel of chemically diverse modified RNAs. The percent HaloTag occupancy is plotted versus time for (A) ct-W, a small molecule, (B) Compound **A-6**, a PS-2′-MOE-modified RNA, (C) Compound **E-2**, a PS-2′-OMe-modified gapmer RNA with a stereopure backbone, (D) Compound **D-6**, a cholesterol-conjugated siRNA, and **E**. Compound **C-11**, a PMO (see SI, Table 1). CAPA data were collected after 2, 4, 8, 24, and 48 h incubation times for the pulse step with the indicated concentrations of the ct-compound. CP_{50} values are listed in SI, Table 9. Error bars show standard error from three independent trials.

transport is not a major barrier for ASO or siRNA effectiveness.[21,22]

We also used CAPA to quantitate the impact of 10% serum on the nuclear penetration of the panel of RNAs after 24 h of incubation. The CP_{50} values in the presence of serum were lower for the PS-modified ASOs **A-6** and **E-2** and for the siRNA **D-6** (SI, Figure 16D,E). While subtle, these differences could affect results for assays that measure knockdown or splice-correcting activity in cell culture.

Measuring the Time Course of Nuclear Penetration. The time course of subcellular trafficking of modified RNA is another critical question in the field. We tested the same panel of compounds in CAPA using AAV-H2GH-transduced cells to quantitate nuclear penetration after incubation for 2, 4, 8, 24, or 48 h in 10% serum (SI Figures 17 and 18). The kinetics of nuclear penetration for the panel of RNA compounds is revealed when the CAPA data are plotted as a function of time, with separate curves for each concentration tested (Figure 4 and SI, Table 9). For small-molecule ct-W, the CAPA signal

saturates within 2 h at concentrations at or above 1.7 μM (Figure 4B), which matches the expectation that ct-W accesses cells passively. The PS-2′-MOE-modified RNA **A-6** and the stereopure PS-2′-OMe gapmer **E-2** require 24 h and micromolar concentrations to saturate the CAPA signal, and nearly no penetration is observed for these ASOs at concentrations of 0.02 μM or lower even after 48 h (Figure 4C,D). By contrast, the siRNA **D-6** does not show substantial penetration until 24 h even at the highest concentration tested (Figure 4E). However, at 24 h, **D-6** is equally or more nuclear penetrant than either of the two ASOs **A-6** and **E-2** (Figure 4E). This finding suggests that some cholesterol-modified siRNAs may have a slower mechanism of uptake and/or endosomal escape than some classes of ASOs, yet the siRNAs may more efficiently escape endosomes at longer time points. Alternatively, the loading of siRNAs onto Ago2 in the cytosol may slow apparent nuclear penetration at shorter time points.

PMO compound **C-11** shows unexpected kinetics of nuclear penetration. **C-11** applied at 1.7 μM showed near-saturation at
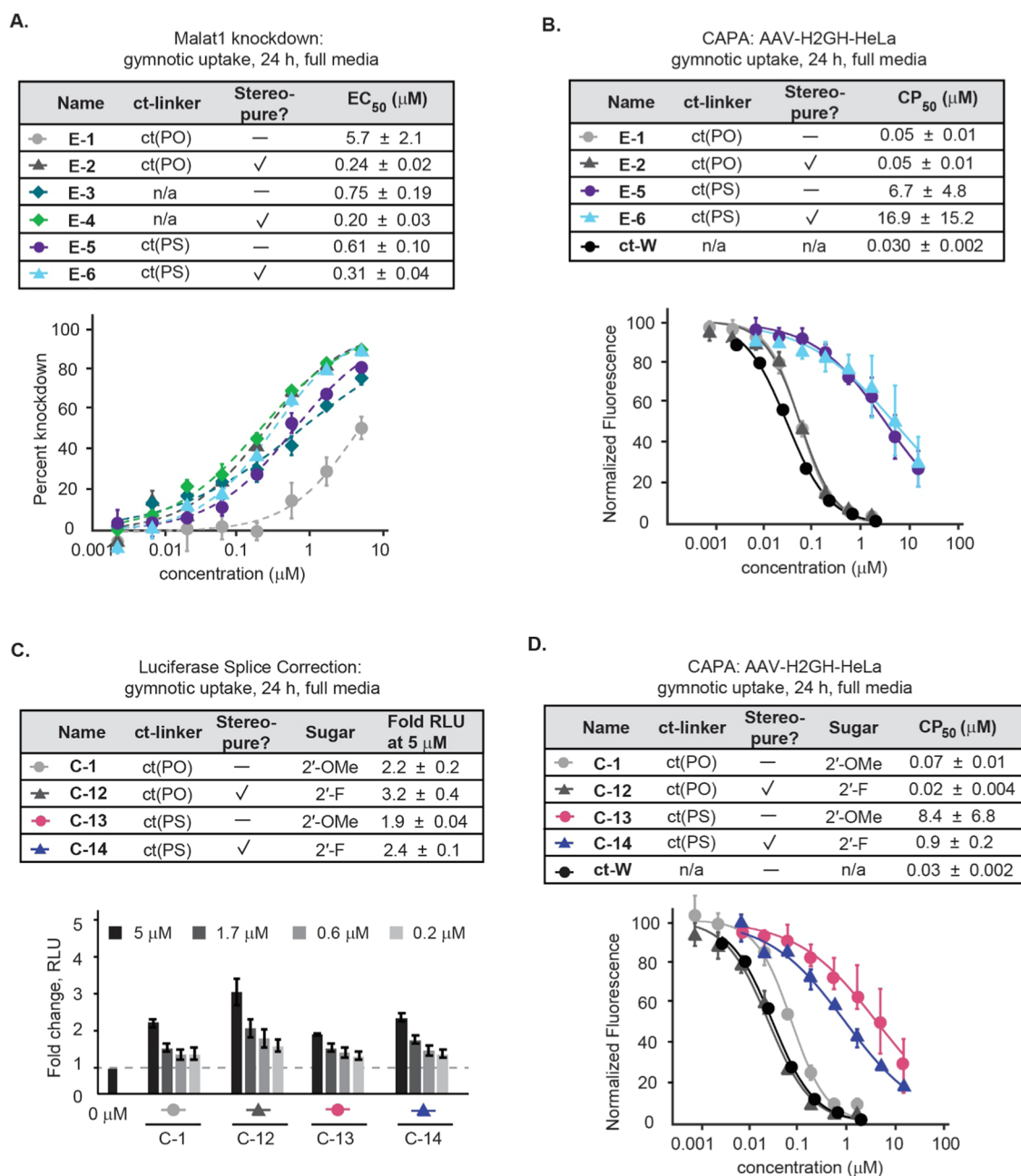
A.

Malat1 knockdown:
gymnotic uptake, 24 h, full media

Name	ct-linker	Stereo-pure?	EC_{50} (μM)
E-1	ct(PO)	—	5.7 ± 2.1
E-2	ct(PO)	✓	0.24 ± 0.02
E-3	n/a	—	0.75 ± 0.19
E-4	n/a	✓	0.20 ± 0.03
E-5	ct(PS)	—	0.61 ± 0.10
E-6	ct(PS)	✓	0.31 ± 0.04

B.

CAPA: AAV-H2GH-HeLa
gymnotic uptake, 24 h, full media

Name	ct-linker	Stereo-pure?	CP_{50} (μM)
E-1	ct(PO)	—	0.05 ± 0.01
E-2	ct(PO)	✓	0.05 ± 0.01
E-5	ct(PS)	—	6.7 ± 4.8
E-6	ct(PS)	✓	16.9 ± 15.2
ct-W	n/a	n/a	0.030 ± 0.002

C.

Luciferase Splice Correction:
gymnotic uptake, 24 h, full media

Name	ct-linker	Stereo-pure?	Sugar	Fold RLU at 5 μM
C-1	ct(PO)	—	2′-OMe	2.2 ± 0.2
C-12	ct(PO)	✓	2′-F	3.2 ± 0.4
C-13	ct(PS)	—	2′-OMe	1.9 ± 0.04
C-14	ct(PS)	✓	2′-F	2.4 ± 0.1

D.

CAPA: AAV-H2GH-HeLa
gymnotic uptake, 24 h, full media

Name	ct-linker	Stereo-pure?	Sugar	CP_{50} (μM)
C-1	ct(PO)	—	2′-OMe	0.07 ± 0.01
C-12	ct(PO)	✓	2′-F	0.02 ± 0.004
C-13	ct(PS)	—	2′-OMe	8.4 ± 6.8
C-14	ct(PS)	✓	2′-F	0.9 ± 0.2
ct-W	n/a	—	n/a	0.03 ± 0.002

Figure 5. Comparing knockdown and splice-correcting activity to CAPA data. (A) *MALAT*1 knockdown activity in HeLa cells. (B) Dose-dependent CAPA curves and CP_{50} values for *MALAT*1 knockdown ASOs. Compounds **E-1** through **E-6** are modified with PS-2′-OMe backbones (SI, Table 1). (C) Splice-correction activity plotted as fold change in luciferase expression over untreated cells, measured in relative luminescence units (RLU). (D) Dose-dependent CAPA curves and CP_{50} values for selected splice-correcting ASOs (SI, Table 1). Cells were incubated with the indicated concentration of the compound for 24 h in media containing 10% serum. Error bars show standard error from three independent trials, and CP_{50} values are reported as average and standard error from three independent curve fits to three independent trials.

8 h (Figure 4F), which is closer to the kinetics observed for the small-molecule ct-W than for the other ASOs **A-6** and **E-2**. However, at concentrations between 0.2 and 1.7 μM, the apparent penetration of **C-11** decreased between 8 and 24 h, indicating less efficient delivery at these time points (Figure 4F). This observation could be due to the fact that the cells are constantly making new HaloTag, but this phenomenon was not observed for any of the other RNAs, small molecules, or peptides tested in CAPA to date.[9,10] Thus, PMOs may undergo multiple mechanisms of penetration with distinct rates of passive penetration, endocytic uptake, and/or endosomal escape. At present, it is unclear whether this is a characteristic

of all PMOs or if it is specific to compound **C-11** or a specific subclass of PMOs.

To integrate both dose dependence and time dependence of the CAPA data, one can derive the minimum concentration and time point required for each compound to achieve nuclear penetration sufficient to saturate CAPA (SI, Table 10). For example, cholesterol-conjugated siRNA **D-6** saturates the CAPA signal at 0.2 μM after 24 h (Figure 4E), whereas at this same concentration, the PMO **C-11** has barely any nuclear localization (Figure 4F). These data are valuable for designing cell-based activity assays at concentrations and time points for
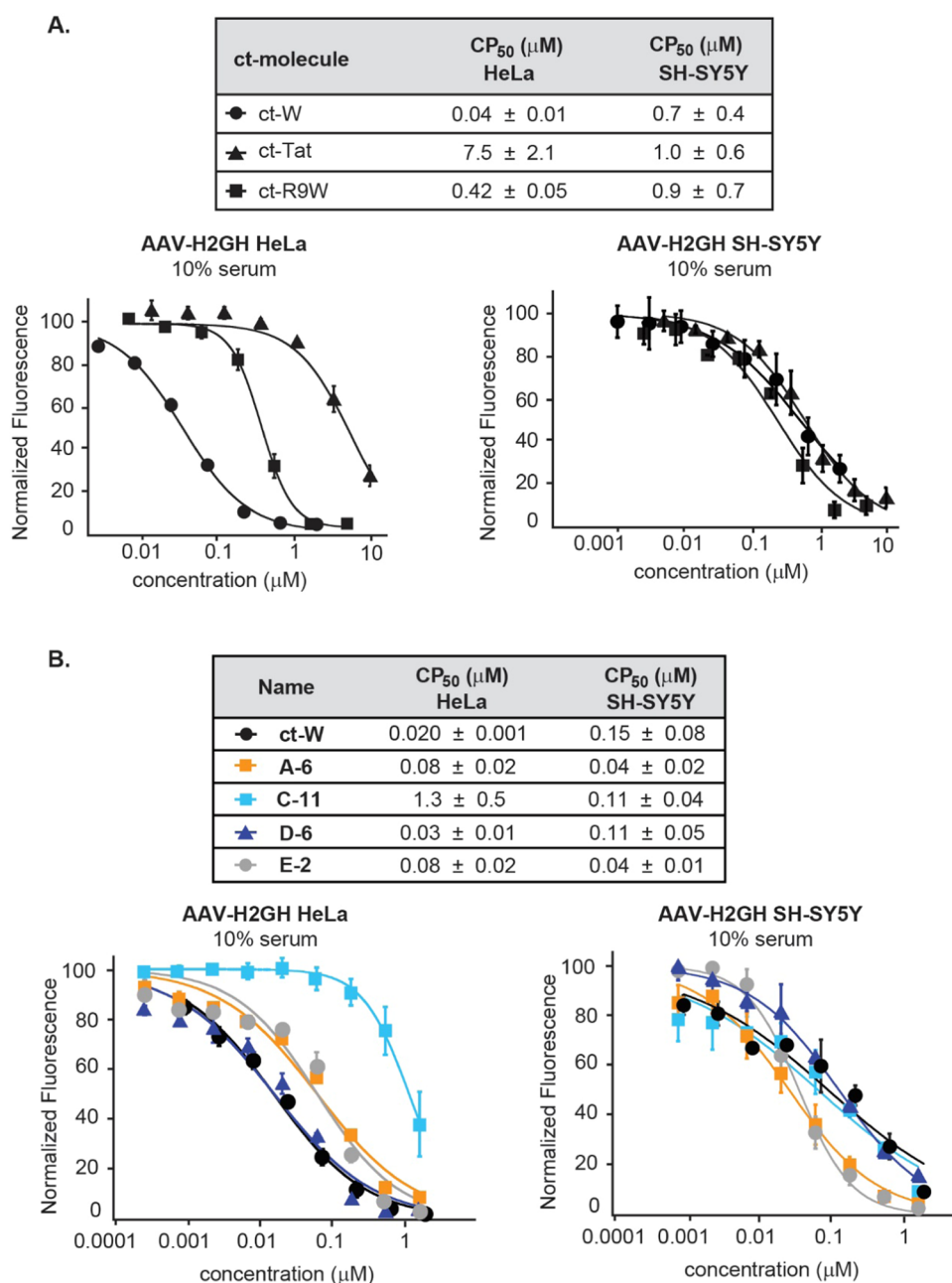
Figure 6. Comparing nuclear penetration in HeLa and SH-SY5Y cells using CAPA. (A) Dose-dependent CAPA data for control compounds using AAV-H2GH-transduced HeLa cells (left panel) or AAV-H2GH-transduced SH-SY5Y cells (right panel). Compounds were incubated for 4 h in OptiMEM with 10% serum. (B) Dose-dependent CAPA data for selected compounds (SI, Table 1) using AAV-H2GH-transduced HeLa cells (left panel) or AAV-H2GH-transduced SH-SY5Y cells (right panel). Compounds were incubated for 24 h in OptiMEM with 10% serum. Significant differences in the CAPA signal were observed between the HeLa and SH-SY5Y cell lines for compounds **A-6**, **E-2**, **D-6**, and **C-11** (p-value <0.05 using a two-tailed t-test). Error bars show standard error from three independent trials, and CP_{50} values are reported as average and standard error from three independent curve fits to three independent trials.

which one can be certain that a substantial amount of the compound is accessing the nucleus.

Effects of Backbone Modifications for RNaseH-Recruiting ASOs. We next sought to understand whether the trends observed for splice-correcting oligonucleotides would also be observed for RNaseH-recruiting oligonucleotides. We prepared ASOs that were designed to knockdown the *MALAT*1 mRNA transcript.[23] These included a PS-2′-OMe gapmer ASO, **E-1**, the corresponding ASO with a stereopure PS backbone in a 5′-SSR-3′ pattern, **E-2**, and non-chloroalkane-labeled analogues of these compounds (**E-3** and

E-4, respectively). Stereopure PS modifications in an SSR pattern were previously shown to enhance activity both *in vitro* and *in vivo*.[24,25] The chloroalkane-tagged compound **E-1** was approximately 8.6-fold less active than its untagged counterpart **E-3**, but the chloroalkane-tagged compound **E-2** was equally active as its untagged counterpart **E-4** (Figure 5A). Consistent with the previous work, the stereopure compounds **E-2** and **E-4** were more active than their stereorandom counterparts, compounds **E-1** and **E-3** (Figure 5A).

Next, we measured nuclear penetration of compounds **E-1** and **E-2** using CAPA with AAV-H2GH-transduced HeLa cells.

The CAPA data showed little difference between the stereorandom and stereopure backbones (Figure 5B, SI, Table 11). In this experiment, we noted that the CP_{50} values for E-1 and E-2 were unusually low and unusually close to that of the small-molecule control ct-W. These CP_{50} values are also lower than one might expect compared to the EC_{50} values observed in the knockdown assays, especially considering that the amount of ASO required to knockdown an mRNA is likely much less than the amount required to block a large proportion of nuclear HaloTag.[10,26,27] These discrepancies could be explained by interference from intracellular mistrafficking, off-target binding, or degradation of chloroalkane-tagged compounds.

Investigating the Effects of Chloroalkane Linker Chemistry. As described in previous work, a drawback of tag-based assays, including fluorescence microscopy and CAPA, is that degradation could release the tag and produce a false-positive signal.[8,9,28] The effects of degradation on assay results are not always thoroughly investigated. The relatively low degree of the CAPA signal for unmodified DNAs (compounds A-1 and B-1, Figure 1 and SI, Figure 6) and the clear dependence of CAPA data on sequence, patterning, and chemical structure indicate that, if there are degradation-induced artifacts, the effects are not independent of uptake and intracellular trafficking. However, the discrepancies between the CAPA data and the knockdown activity data for compounds E-1 and E-2 suggested that there might be at least some degree of CAPA signal that is dependent on a nonproductive uptake or degradation pathway.

Prior work has established that chemically modified oligonucleotides similar to those used here are quite stable to degradation in cell culture for at least 24 h.[15,29] We identified the 5′ phosphodiester group, which was used to link PS-modified oligonucleotides to the chloroalkane tag, as a possible liability. To examine whether the 5′ phosphodiester might be labile in cells, we prepared versions of E-1 and E-2 with chloroalkanes linked via a 5′ phosphorothiodiester group instead of a 5′ phosphodiester (compounds E-5 and E-6). We refer to these chloroalkane tags as ct(PS) and ct(PO), respectively (SI, Figure 19A). In the *malat*1 knockdown assay, the ct(PS)-linked ASOs E-5 and E-6 had similar or improved activity compared to their corresponding ct(PO)-linked ASOs E-1 and E-2 (Figure 5A). However, in CAPA measuring nuclear localization, compounds with the ct(PS) linker required over 100-fold higher concentrations to block cytosolic HaloTag (Figure 5B). The higher CP_{50} values for the ct(PS)-linked ASOs compared to the ct(PO)-linked ASOs were in stark contrast to their similar *malat*1 knockdown activities, but the CP_{50} values were more consistent with expectations given the relative sensitivities of the knockdown assay and CAPA.[10,26,27] Similar trends were observed for splice-correcting ASOs with ct(PO) and ct(PS) linkers (SI, Figures 20−21 and SI, Table 1). Overall, these data suggest that compounds with a ct(PO) linker produce CAPA data where some of the signal is due to nonproductive uptake and/or release of the chloroalkane tag, for example, due to degradation in the endolysosomal compartment. These observations match recent work which showed that a single phosphodiester bond represented a similar liability for aptamer-drug conjugates.[30] These findings support the hypothesis that oligonucleotides with a single phosphodiester linkage should be avoided in favor of exclusively phosphorothiodiester linkages.

Investigating Penetration in a Neuronal Cell Line. Using AAVs to introduce HaloTag unlocks the potential to perform CAPA in non-HeLa cell lines, which has never been done before. To demonstrate this capability, we used AAV-H2GH vectors to perform CAPA in SH-SY5Y neuroblastoma cells. Expression and distribution of Histone2B-GFP-HaloTag were similarly robust in SH-SY5Y cells as for HeLa cells (SI, Figure 22). We tested nuclear penetration of control compounds ct-W, ct-Tat, and ct-R9W in SH-SY5Y cells and observed very different trends compared to HeLa cells (Figure 6A). We then tested a panel of chemically modified RNAs in SH-SY5Y cells (Figure 6B). The two phosphorothioate-modified ASOs, compounds A-6 and E-2, had similar nuclear penetration in both cell lines, but the small-molecule ct-W and the siRNA D-6 were approximately 3-to-5-fold less penetrant in SH-SY5Y than in HeLa (Figure 4B). Interestingly, the PMO compound C-3 was much less cell penetrant than the other ASOs in HeLa but comparable to the other ASOs in SH-SY5Y (Figure 6B). These results for small molecules, peptides, ASOs, and siRNAs underscore that performing CAPA in different cell lines will be very valuable for understanding cell- and tissue-specific penetration for many drug classes.

■ CONCLUSIONS

In this work, we applied CAPA to measure the cytosolic and nuclear penetration of chemically modified oligonucleotides. CAPA data for oligonucleotide therapeutics with clinically relevant sequences and chemical modifications follow the general trends observed in the literature for activity.[18,31−33] For ASOs, our data suggest that the cytosolic penetration of PS-2′-OMe ASOs is generally slightly more favorable than that of PS-2′-MOE ASOs for several, but not all, modification patterns. For siRNAs, our data matched previous work using cholesterol-conjugated siRNAs which suggested that increasing overall PS content in an siRNA correlates to an increase in cellular uptake and activity,[17,19,34] at least for siRNAs labeled with chloroalkane on the sense strand.

For oligonucleotide therapeutics, knockdown or splice-correcting activity is typically observed after days or weeks of exposure, a phenomenon that has been explained by a relatively slow rate of endosomal escape in target tissues.[3−5] The time course data (Figure 4) show that nuclear penetration can occur in 2−8 h for some compounds, while others take at least 24 h to show substantial nuclear penetration. These results, plus some unusual internalization kinetics observed for a PMO, may suggest that some oligonucleotide therapeutics have a uniquely slow endosomal release mechanism or potentially multiple release mechanisms with different rates.

As with any tag-based assay, including common uptake assays involving dye-conjugated oligonucleotides, the tag may have an effect on compound internalization and endosomal escape.[8,35] In our control experiments, we documented specific effects of the chloroalkane tag on ASOs and siRNAs. Despite these observations, we note that CAPA-derived CP_{50} values were not unusually low for control DNA oligonucleotides, which are much more prone to degradation. We also observed several siRNAs with phosphodiester linkages that showed almost no CAPA signal at all even at 48 h time points (Figure 3B). Even for compounds with 5′ phosphodiester linkages, the CAPA signal varied widely based on the chemical modifications, patterning, and sequences (Figures 1−2, SI Figures 6−8, and 16−18). Additionally, a 24 h incubation in full medium did not show substantial degradation of compounds with 5′

phosphodiester linkages (SI, Figure 23). Interestingly, there was little difference in CAPA data between ASOs with a 5′ phosphodiester linker and a 5′ phosphorothiodiester linker in SH-SY5Y cells (SI, Figure 24 and SI, Table 11). Altogether, these data imply that CAPA is not being affected by rapid degradation in the extracellular environment, and that any nonproductive uptake process that is detected by CAPA represents endosomal, lysosomal, or cytosolic events that are relevant for understanding the intracellular trafficking of oligonucleotide therapeutics. Future work could carefully explore other linker chemistries to examine their fates in different cell lines. For example, we used dibenzocyclooctyne-based chloroalkane reagents[10] to produce analogues of compounds **A-6**, **B-4**, and **C-11**, and these enhanced the apparent cytosolic penetration of the PS-modified ASOs but not the PMO (SI, Figure 25 and SI, Table 14). Our data emphasize the importance of careful controls for the chemistry and placement of any tag conjugated to the oligonucleotide, not just for CAPA but for all tag-based assays.

Overall, CAPA sheds light on one part of the complex pathways that govern the uptake and subcellular trafficking of oligonucleotide therapeutics. Moving forward, CAPA will be very valuable for screening RNAs with novel chemistries, especially when applied directly to the most therapeutically relevant cell types.

■ METHODS

Synthesis of Chloroalkane-Carboxylic acid. The structure of the chloroalkane-carboxylic acid tag is shown in SI, Figure 1. The synthesis of the chloroalkane-carboxylic acid tag was performed, as previously described.[9,10] The final product was confirmed by MALDI-TOF mass spectrometry (expected m/z: 323.8 g/mol) and ^{1}H NMR.

Synthesis of Chloroalkane-Dibenzocyclooctyne. The structure of the chloroalkane-dibenyzocyclooctyne (ct-DBCO) tag is shown in SI, Figure 1. The chloroalkane-amine is an intermediate of the established protocol for the synthesis of the chloroalkane-carboxylic acid.[9,10] Chloroalkane-amine was purified by preparatory RP-HPLC on a C18 column using a gradient of water and acetonitrile with 0.1% trifluoroacetic acid. The final product was confirmed by MALDI-TOF mass spectrometry (expected m/z: 223.9 g/mol) and ^{1}H NMR. Purified chloroalkane-amine (2 equiv) was incubated with 1 equiv dibenzocyclooctyne-NHS (Sigma) and 5 equiv diisopropylethylamine (DIPEA) in 1 mL of dry N,N-dimethylformamide (DMF). The reaction mixture was incubated for 4 h at room temperature with shaking, diluted with water, and purified by RP-HPLC. The identity of the final product was confirmed by MALDI-TOF mass spectrometry (expected m/z: 511.1 g/mol) and ^{1}H NMR.

Synthesis of Chloroalkane-TMR. Chloroalkane-tetramethylrhodamine (ct-TMR) was synthesized, as described previously.[9,10] Briefly, tetramethylrhodamine-N-hydroxysuccinimide (1 equiv) was added to chloroalkane-amine (2 equiv) with DIPEA (2.5 equiv) in DMF. The reaction mixture was stirred at room temperature overnight, diluted with water, and purified by RP-HPLC. The identity of the final product was confirmed by MALDI-TOF mass spectrometry (expected m/z: 636.2 g/mol).

Synthesis of Stereorandom and Stereopure Oligonucleotides. Stereorandom phosphodiester (PO) and phosphorothioate (PS) oligonucleotides were synthesized on a solid support using standard methodologies. Oligonucleotides from the sequence A series and the sequence B series were prepared by Integrated DNA Technologies. We synthesized and purified chemically modified stereopure oligonucleotides as described,[24,25] using synthetic cycles of (1) detritylation using 3% trichloroacetic acid in dichloromethane, (2) coupling using 0.2 M monomer in 20% isobutyronitrile-acetonitrile and then 0.5 M N-cyanomethylimidazolium triflate in acetonitrile, (3) oxidation, for PO, using 50 mM I_2/pyridine-H_2O and sulfurization, or for PS, using xanthane hydride, and (4) capping using

20% Ac$_2$O, 30% 2,6-lutidine in acetonitrile and then 20% N-methylimidazole in acetonitrile. After synthesis, the column was washed with 2 mL of 20% diethylamine in acetonitrile for 12 min. Oligonucleotides on the solid support were transferred from the synthesis column to a Falcon tube and 2.5 mL of HF solution (5% triethylamine-3HF, 7% triethylamine, 14.7% water, 73.3% DMSO; v/v) was added. The mixture was shaken at 28 °C for 3 h. Concentrated ammonia solution (5 mL) was added to this mixture; the mixture was shaken at 37 °C for 24 h, and then, the mixture was filtered to isolate the crude oligonucleotide.

Synthesis of Lipid-Conjugated siRNAs. All siRNA compounds were synthesized and characterized by Biosynthesis Inc.

Conjugation of Chloroalkane to Oligonucleotides. Oligonucleotides were prepared with a 5′ amine with a six-carbon linker. Oligonucleotides were dissolved in nuclease-free water to a stock concentration of 10 mM. In relation to the oligonucleotide, 10 equiv of chloroalkane-carboxylic acid was dissolved in 60 μL of MES buffer (pH 6.0) along with 10 equiv of EDC and 20 equiv of sulfo-NHS. The reaction mixture was incubated for 20 min at room temperature with shaking to activate carboxylic acid. Then, the 5′ amine-oligonucleotide was added to the reaction mixture. A solution of 0.5 M NaHCO$_3$ was added until the solution reached a pH between 7.0 and 8.0, and nuclease-free water was added to bring the solution up to 100 μL total. The reaction was incubated overnight at room temperature with shaking and then purified by RP-HPLC using a C18 analytical column. The mobile phase was a gradient of 95% Solvent A (5% acetonitrile in aqueous 100 mM triethylammonium acetate, TEAAc) and 5% Solvent B (20% solvent A with 80% acetonitrile) to 100% Solvent B over 20 min. Chloroalkane-tagged oligonucleotides were purified to at least 95% purity, identity was confirmed by MALDI-TOF mass spectrometry, and purified stocks were desalted, lyophilized, and stored at −20 °C.

For chloroalkane-tagged ASOs, synthetic oligonucleotides with a 5′ amine were conjugated with chloroalkane, as described above. The mobile phase was a gradient of 95% Solvent A (5% acetonitrile in aqueous 50 mM sodium acetate) to 100% Solvent B (10% of solvent A with 90% acetonitrile in 50 mM sodium acetate) over 20 min. Chloroalkane-tagged oligonucleotides were purified to at least 95% purity, identity was confirmed by MALDI-TOF mass spectrometry, and purified stocks were desalted, lyophilized, and stored at −20 °C. For annealing, the modified sense strand was combined with a corresponding antisense strand in a 1:1 ratio in 1 mM MgCl$_2$, vortexed for 10 s, centrifuged for 10 s, and heated at 90 °C for 5 min. The solution was cooled slowly to 4 °C over the course of approximately 2 h. For preparing siRNAs attached to a chloroalkane using click chemistry, sense strands labeled with a 5′ azide were incubated with chloroalkane-DBCO in aqueous 100 mM TEAAc overnight at room temperature with shaking. Sense strands were purified and annealed, as described above.

For preparing the chloroalkane-tagged oligonucleotides from the sequence E series, 3 equiv of chloroalkane-carboxylic acid was dissolved in DMF with 10 equiv of DIPEA and 2.4 equiv of HATU. The reaction mixture was shaken at room temperature for 30 min. The activated choloralkane tag was added into a solution of 5′ amino-oligonucleotide in 75% DMSO and 25% water. The reaction mixture was shaken at room temperature for 2 h, and the extent of reaction was monitored by LC-MS. Upon completion of the reaction, the mixture was diluted with 10 mL of water. The crude mixture was purified by RP-HPLC using a preparatory-scale C8 column. The mobile phase was a gradient of 95% Solvent A (aqueous 50 mM TEAAc) and 5% Solvent B (acetonitrile) to 40% solvent B over 30 min. Pure fractions were collected and desalted by size-exclusion chromatography on an AKTA purifier. Pure oligonucleotides were concentrated and filtered using a 0.2 μm nylon filter. The final product was characterized using LC-MS and UPLC.

Cell Culture and Maintenance. HeLa cells were grown in DMEM supplemented with 10% fetal bovine serum (FBS). The HaloTag-GFP-mito (HGM) cells used for cytosolic CAPA were grown in DMEM supplemented with 10% fetal bovine serum (FBS), 1% penicillin/streptomycin, and 1 μg/mL puromycin. When

necessary, HGM cells were selected with 20 μg/mL puromycin. The HeLa cells used for the luciferase splicing assays (HeLa-Luc705) were grown in DMEM supplemented with 10% fetal bovine serum (FBS). When necessary, HeLa-Luc705 cells were selected with 200 μg/mL hygromycin B. All HeLa cell lines were kept at 37 °C with 5% CO2 and passaged every 2−3 days prior to confluency. SH-SY5Y cells were grown in a 1:1 ratio of EMEM to F12 media supplemented with 10% FBS. SH-SY5Y cells were kept at 37 °C with 5% CO2 and passaged every 4−6 days.

Chloroalkane Penetration Assay (CAPA). CAPA was performed as described previously on adhered HGM cells in a 96-well tissue culture treated plate.[9,10] Briefly, compounds were incubated with cells at 37 °C in optiMEM or optiMEM with 10% FBS for the desired incubation time to allow for internalization. Cells were washed with 50 μL of fresh optiMEM for 15 min, chased with 50 μL of 5 μM ct-TMR for 15 min, and then washed with fresh optiMEM for 30 min. After the washes, cells were trypsinized with 40 μL of 0.05% clear trypsin, resuspended in 180 μL of PBS, and then analyzed by flow cytometry, as described.[9,10] For all CAPA experiments, three independent trials were performed and data points are shown as averages with error bars representing the standard error of the mean from the three independent trials. All CP_{50} values are reported as averages and standard errors from three independently calculated curve fits from the three independent trials.

Luciferase Reporter Assay for Spice-Switching. The splice-switching reporter cell line was a HeLa cell line that stably expresses a pre-mRNA transcript of the luciferase gene interrupted by a β-globin mRNA sequence, as described previously.[16] This cell line is referred to as HeLa-Luc705 and was obtained from the UNC Tissue Culture Facility. Sequence C oligonucleotides were designed to correct splicing for this reporter, resulting in luciferase expression.[16] HeLa-Luc705 cells were seeded in 96-well tissue culture treated plates at a density of 1.2×10^4 cells per well. At the start of the experiment, the cells were treated with serial dilutions of oligonucleotides in 100 μL of optiMEM and then incubated at 37 °C for either 24 or 48 h. After the incubation period, cells were washed with fresh optiMEM for 15 min and then washed with PBS for 15 min. Cells were lysed directly in the 96-well plate with 50 μL of the 1× cell culture lysis reagent (Promega). Luciferase assay reagent (55 μL) was added (Promega), samples were mixed well by pipetting and then incubated for 2 min at room temperature. Luciferase activity was measured in relative luminescence units (RLU) with a Tecan Spark plate reader. The RLU value for each sample was used to calculate a fold change compared to the control, untreated cells.

Malat1 Knockdown Experiments. HeLa cells were seeded in 96-well tissue culture treated plates at a density of 1.5×10^4 cells per well and allowed to adhere overnight. At the start of the experiment, the cells were treated with serial dilutions of sequence E oligonucleotides in full growth media and then incubated at 37 °C for 24 h. After 24 h, the RNA was extracted using the SV96 Total RNA Isolation System (Promega) following the manufacturer's instructions. In brief, cells were collected in RNA lysis buffer and passed through the extraction column. Columns were washed once and then on-column DNase treatment was carried out for 10 min. DNA Stop buffer was used to quench the DNase, and the column was washed again. Total RNA was eluted in distilled deionized water. Reverse transcription was achieved using the High-Capacity RNA to cDNA kit (Applied Biosystems-4387406) following the manufacturer's instructions. Briefly, RT buffer and enzyme were diluted to 1× with RNA and water, and the reaction was incubated at 37 °C for 60 min and then 95 °C for 5 min. cDNA was stored at −20 °C until used. Quantification of MALAT1 abundance was performed in duplicate using iQ Multiplex Powermix (Bio-Rad) following the manufacturer's instructions. In brief, iQ buffer and probesets for MALAT1 and SRSF9 were diluted in water, and 2 μL of cDNA from the above reaction was added. The reaction was then incubated at 95 °C for 3 min followed by cycling between 95 °C for 10 s and 60 °C for 30 s. Cycling was terminated after 40 cycles. The delta-delta-CT method was used to quantify MALAT1, normalizing to the control gene SRSF9 and to mock treated control samples. The following

probesets were used for quantification: MALAT1 (Applied Biosystems, hs00273907-FAM/NFQ), SRSF9: Custom Probeset (Integrated DNA Technologies, Forward: TGGAATATGCCCTGCG-TAAA, Reverse: TGGTGCTTCTCTCAGGATAAAC, Probe: TGGATGACACCAAATTCCGCTCTCA-HEX/NFQ)

HPRT Knockdown Experiments. For siRNA delivery facilitated by transfection, an 11-point siRNA concentration range was created by 1:3 serial dilution of a 16 nM siRNA solution in OptiMEM. The diluted siRNA (25 μL) was added to 25 μL of Lipofectamine RNAiMax in OptiMEM (0.3 μL of RNAiMax and 24.7 μL of OptiMEM per well) and the mixture was incubated for 10 min at room temperature. In the meantime, HeLa cells were washed, trypsinized, spun down, resuspended in media, and diluted to 3×10^5 cells per mL. This cell mixture (50 μL) was added to the siRNA-RNAiMax mixture and cells were incubated for 24 h at 37 °C. The cells were washed twice with PBS and the plate was tapped dry. The plates were processed using the fast Cells-to-CT kit following the TaqMan Fast Advanced Cells-to-CT protocol (ThermoFisher). In the qPCR protocol, GapDH FAM (Hs99999905_m1) and HPRT FAM (Hs02800695_m1) were used as gene assays.

For passive uptake, HeLa cells were split at 5×10^3 cells per well in cell culture media (DMEM with 10% FBS and 1% penicillin/streptomycin solution) and cells were incubated for 24 h at 37 °C. Cells were washed twice with PBS. An 11-point concentration range was created by 1:3 serial dilution of 400 nM siRNA in Accell media. Each dilution (150 μL) of each siRNA was added to the wells. Cells were incubated at 37 °C for 72 h. Cells were washed twice with PBS and the plate was tapped dry. The plates were processed using the fast Cells-to-Ct kit following the Fisher TaqMan Fast Advanced Cells-to-CT protocol (ThermoFisher). In the qPCR protocol, GapDH FAM (Hs99999905_m1) and HPRT FAM (Hs02800695_m1) were used as gene assays.

T_m Measurements. siRNA was diluted to 2 μM in 0.1× PBS in a 96-well plate. EvaGreen Dye (2000× in DMSO) was diluted at 1:1000 in 0.1× PBS. The dye (5 μL) was added to wells in a 384-well plate. siRNA (5 μL) was added to each well, each sample was added in 4 wells to create 4 replicates per sample. The plate was covered, briefly vortexed, and spun down (1 min, 1200 rpm) before putting the sample in a QS7 (ThermoFisher). The samples were run according to an adjusted melting temperature program.

LightCycler stage	temp (°C)	acquisition mode	hold (s)	ramp rate (°C/S)
Denaturation	95		60	1.91
Annealing	25		60	1.65
Premelting	32		1	1.91
Melting	95	Continuous		0.05
Cooling	40		30	1.65

Cell Lysate Spike-in RISC Loading. The methods to analyze RISC loading were developed based on the methods previously described by Pei et al.,[36] with modifications. Briefly, 5×10^5 HeLa cells were added to a 1.5 mL Eppendorf tube and spun at 500 g for 5 min. Cells were lysed in lysate buffer (50 mM Tris-HCl at pH 7.5, 200 mM NaCl, 0.5% Triton-x-100) with the addition of protease and phosphatase inhibitors (ThermoFisher 78446) and Superase RNAse inhibitor (ThermoFisher AM2694). siRNA was spiked into the lysate at a 4 nM concentration and incubated at 37 °C for 4 h with agitation every hour. Lysates containing siRNA were then spun at 4 °C at 16 000 g for 10 min. A Pierce BCA protein assay (ThermoFisher 23225) was performed to determine the amount of protein present. An AGO2 immunoprecipitation was executed using the manufacturer's protocol with small modifications. Dynabead protein G magnetic beads (ThermoFisher 10004D) were incubated with 1 μg of the AGO2 antibody (Wako FujiFilm 011-22033) at 4 °C for 30 min. Beads were washed once with antibody binding buffer (PBS with 0.02% Tween-20) and 75 μg of protein was incubated with the antibody-bound beads at 4 °C for 30 min. Following three washes with lysis buffer, AGO2 was eluted with elution buffer (ThermoFisher 21028). Stem loop qPCR using the small RNA assay design (ThermoFisher 4398987) specific to the HPRT-antisense and

mir16 (ThermoFisher Assay ID 000391) were performed using 5 μL of eluted AGO2. Standard curves for the HPRT-antisense strand and mir16 were prepared with single-stranded oligos (1000−0.001 pg/μL) to determine the concentration of strand loaded into AGO2. Results were normalized to the amount of mir16 to account for any variability in the AGO2 immunoprecipitation.

AAV Plasmid Preparation and Transduction. The AAV plasmid that produces a cytosolic HaloTag is referred to as AAV-ITR-HGM, representing an AAV-compatible plasmid with a HaloTag-GFP-Mito fusion as the transgene (mito is a peptide that targets the fusion to the outside of the outer mitochondrial membrane).[11] First, the HaloTag-GFP-Mito portion of plasmid pERB254 (Addgene 67762) was amplified using PCR. The HaloTag-GFP-Mito was inserted into the AAV vector (AAV-CMV-GFP,9 Addgene 67634) via Gibson assembly. Correct insertion was verified with a restriction digest using *Bss*HII. The AAV construct to generate a nucleus-localized HaloTag is referred to as AAV-ITR-H2GH, representing an AAV-compatible plasmid with a Histone2B-GFP-HaloTag fusion as the transgene. This plasmid was made by amplifying the HaloTag-encoding portion of plasmid pERB254 (Addgene 67762) and then inserting it in-frame within a vector encoding Histone2B-GFP (Addgene 11680) using Gibson assembly. The Histone2B-GFP-HaloTag fusion was then amplified using PCR and inserted into the AAV vector (AAV-CMV-GFP,9 Addgene 67634) using Gibson assembly. Correct insertion was verified with a restriction digest. Plasmids for AAV packaging were prepared using a MaxiPrep plasmid purification kit (Qiagen) and constructs were packaged into AAV2 viral particles by the Salk Institute (San Diego, CA). See SI, Figure 10 and SI, Figure 11 for the plasmid map and open reading frame sequence of AAV-HGM. See SI, Figure 12 and SI, Figure 13 for the plasmid map and open reading frame sequence of AAV-H2GH.

For viral transduction, HeLa cells were seeded in a 96-well plate at a density of 1.2×10^4 cells per well the day before the experiment. AAV2 particles were added at a MOI of 1×10^4 using a stock of 10^{12} copies/mL AAV premixed in growth media. The HeLa cells were incubated with AAV2 at 37 °C for 3 h, after which media was exchanged. Cells were tested in CAPA at 24, 48, or 72 h after transduction. SH-SY5Y cells were seeded in a 96-well plate at a density of 1.5×10^4 cells per well the day before the experiment. AAV2 particles were added at an MOI of 10^4 using a stock of 10^{12} copies/mL AAV premixed in growth media. The SH-SY5Y cells were incubated with AAV2 at 37 °C for 24 h, and then, CAPA was performed on the transduced cells.

Oligonucleotide Degradation Assay. Two ct-ASOs with the base sequence of nusinersen (Sequence A: UCACUUUCAUAAUG-CUGG) were prepared, one synthesized with a ct(PO) linker and one with a ct(PS) linker. Each ct-ASO (35 μM) was incubated in PBS, OptiMEM, or full growth media for 24 h at 37 °C. Samples were analyzed by analytical RP-HPLC using an XBridge Oligonucleotide BEH C18 column with a gradient of 95% solvent A (5% acetonitrile in 0.1M aqueous triethylammonium-acetic acid at pH 7) and 5% solvent B (80% acetonitrile in 0.1M aqueous triethylammonium-acetic acid at pH 7) to 100% solvent B over 20 min. The peak area of intact ct-ASO integrated for each HPLC trace at 24 h in each condition was compared to the peak area from the initial time point at 0 h to obtain the percent intact ct-ASO remaining. All assays were performed with three independent trials.

ASSOCIATED CONTENT

Ⓢ Supporting Information

The Supporting Information is available free of charge at https://pubs.acs.org/doi/10.1021/acschembio.1c00830.

> Structures and/or sequences and characterization of all compounds, primary data from CAPA and other assays, and additional data sets referred to in the manuscript (PDF)

■ AUTHOR INFORMATION

Corresponding Author
Joshua A. Kritzer − *Department of Chemistry, Tufts University, Medford, Massachusetts 02155, United States;* ⊙ orcid.org/0000-0003-2878-6781; Email: joshua.kritzer@tufts.edu

Authors
Kirsten Deprey − *Department of Chemistry, Tufts University, Medford, Massachusetts 02155, United States*

Nefeli Batistatou − *Department of Chemistry, Tufts University, Medford, Massachusetts 02155, United States*

Marjoke F. Debets − *Lilly Research Laboratories, Eli Lilly and Company, Indianapolis, Indiana 46285, United States*

Jack Godfrey − *Wave Life Sciences, Cambridge, Massachusetts 02138, United States*

Kirstin B. VanderWall − *Lilly Research Laboratories, Eli Lilly and Company, Indianapolis, Indiana 46285, United States*

Rebecca R. Miles − *Lilly Research Laboratories, Eli Lilly and Company, Indianapolis, Indiana 46285, United States*

Livia Shehaj − *Department of Chemistry, Tufts University, Medford, Massachusetts 02155, United States*

Jiaxing Guo − *Department of Chemistry, Tufts University, Medford, Massachusetts 02155, United States*

Amy Andreucci − *Wave Life Sciences, Cambridge, Massachusetts 02138, United States*

Pachamuthu Kandasamy − *Wave Life Sciences, Cambridge, Massachusetts 02138, United States*

Genliang Lu − *Wave Life Sciences, Cambridge, Massachusetts 02138, United States*

Mamoru Shimizu − *Wave Life Sciences, Cambridge, Massachusetts 02138, United States*

Chandra Vargeese − *Wave Life Sciences, Cambridge, Massachusetts 02138, United States*

Complete contact information is available at:
https://pubs.acs.org/10.1021/acschembio.1c00830

Notes

■ REFERENCES

(1) Kaczmarek, J. C.; Kowalski, P. S.; Anderson, D. G. Advances in the delivery of RNA therapeutics: from concept to clinical reality. *Genome Med.* **2017**, *9*, 60−76.

(2) Engelhardt, J. A. Comparative Renal Toxicopathology of Antisense Oligonucleotides. *Nucleic Acid Ther.* **2016**, *26*, 199−209.

(3) Johannes, L.; Lucchino, M. Current Challenges in Delivery and Cytosolic Translocation of Therapeutic RNAs. *Nucleic Acid Ther.* **2018**, *28*, 178−193.

(4) Crooke, S. T.; Wang, S.; Vickers, T. A.; Shen, W.; Liang, X. Cellular uptake and trafficking of antisense oligonucleotides. *Nat. Biotechnol.* **2017**, *35*, 230−237.

(5) Juliano, R. L. Intracellular Trafficking and Endosomal Release of Oligonucleotides: What We Know and What We Don't. *Nucleic Acid Ther.* 2018, 28, 166−177.

(6) Soifer, H. S.; Koch, T.; Lai, J.; Hansen, B.; Hoeg, A.; Oerum, H.; Stein, C. A. Silencing of Gene Expression by Gymnotic Delivery of Antisense Oligonucleotides. In *Methods in Molecular Biology*, 2012; Vol. 815, pp 333−346.

(7) Deprey, K.; Batistatou, N.; Kritzer, J. A. A critical analysis of methods used to investigate the cellular uptake and subcellular localization of RNA therapeutics. *Nucleic Acids Res.* 2020, 48, 7623−7639.

(8) Lacroix, A.; Vengut-Climent, E.; De Rochambeau, D.; Sleiman, H. F. Uptake and Fate of Fluorescently Labeled DNA Nanostructures in Cellular Environments: A Cautionary Tale. *ACS Central Sci.* 2019, 5, 882−891.

(9) Peraro, L.; Deprey, K. L.; Moser, M. K.; Zou, Z.; Ball, H. L.; Levine, B.; Kritzer, J. A. Cell Penetration Profiling Using the Chloroalkane Penetration Assay. *J. Am. Chem. Soc.* 2018, 140, 11360−11369.

(10) Deprey, K.; Kritzer, J. A. Quantitative Measurement of Cytosolic Penetration Using the Chloroalkane Penetration Assay. In *Methods in Enzymology*, 2020; Vol. 641, pp 277−309.

(11) Ballister, E. R.; Aonbangkhen, C.; Mayo, A. M.; Lampson, M. A.; Chenoweth, D. M. Localized light-induced protein dimerization in living cells using a photocaged dimerizer. *Nat. Commun.* 2014, 5, No. 5475.

(12) Los, G. V.; Encell, L. P.; Mcdougall, M. G.; Hartzell, D. D.; Karassina, N.; Zimprich, C.; Wood, M. G.; Learish, R.; Ohana, R. F.; Urh, M.; Simpson, D.; et al. HaloTag: A Novel Protein Labeling Technology for Cell Imaging and Protein Analysis. *ACS Chem. Biol.* 2008, 3, 373−382.

(13) Claborn, M. K.; Stevens, D. L.; Walker, C. K.; Gildon, B. L. Nusinersen: A Treatment for Spinal Muscular Atrophy. *Ann. Pharmacother.* 2019, 53, 61−69.

(14) Marafini, I.; Monteleone, G. Inflammatory bowel disease: new therapies from antisense oligonucleotides. *Ann. Med.* 2018, 50, 361−370.

(15) Khvorova, A.; Watts, J. K. The chemical evolution of oligonucleotide therapies of clinical utility. *Nat. Biotechnol.* 2017, 35, 238−248.

(16) Kang, S.-H.; Cho, M.-J.; Kole, R. Up-Regulation of Luciferase Gene Expression with Antisense Oligonucleotides: Implications and Applications in Functional Assay Development. *Biochemistry* 1998, 37, 6235−6239.

(17) Bramsen, J. B.; Laursen, M. B.; Nielsen, A. F.; Hansen, T. B.; Bus, C.; Langkjær, N.; Babu, B. R.; Højland, T.; Abramov, M.; Van Aerschot, A.; et al. A large-scale chemical modification screen identifies design rules to generate siRNAs with high activity, high stability and low toxicity. *Nucleic Acids Res.* 2009, 37, 2867−2881.

(18) Stanton, R.; Sciabola, S.; Salatto, C.; Weng, Y.; Moshinsky, D.; Little, J.; Walters, E.; Kreeger, J.; Dimattia, D.; Chen.; et al. Chemical Modification Study of Antisense Gapmers. *Nucleic Acid Ther.* 2012, 22, 344−359.

(19) Osborn, M. F.; Khvorova, A. Improving siRNA Delivery In Vivo Through Lipid Conjugation. *Nucleic Acid Ther.* 2018, 28, 128−136.

(20) Coles, A. H.; Osborn, M. F.; Alterman, J. F.; Turanov, A. A.; Godinho, B. M. D. C.; Kennington, L.; Chase, K.; Aronin, N.; Khvorova, A. A High-Throughput Method for Direct Detection of Therapeutic Oligonucleotide-Induced Gene Silencing In Vivo. *Nucleic Acid Ther.* 2016, 26, 86−92.

(21) Lorenz, P.; Misteli, T.; Baker, B. F.; Bennett, C. F.; Spector, D. L. Nucleocytoplasmic shuttling: a novel in vivo property of antisense phosphorothioate oligodeoxynucleotides. *Nucleic Acids Res.* 2000, 28, 582.

(22) Juliano, R. L.; Ming, X.; Nakagawa, O. Cellular uptake and intracellular trafficking of antisense and siRNA oligonucleotides. *Bioconjugate Chem.* 2012, 23, 147−157.

(23) Arun, G.; Aggarwal, D.; Spector, D. L. MALAT1 Long Non-Coding RNA: Functional Implications. *Non-coding RNA* 2020, 6, No. 22.

(24) Iwamoto, N.; Butler, D. C. D.; Svrzikapa, N.; Mohapatra, S.; Zlatev, I.; Sah, D. W. Y.; Meena; Standley, S. M.; Lu, G.; Apponi, L. H.; et al. Control of phosphorothioate stereochemistry substantially increases the efficacy of antisense oligonucleotides. *Nat. Biotechnol.* 2017, 35, 845−851.

(25) Liu, Y.; Dodart, J. C.; Tran, H.; Berkovitch, S.; Braun, M.; Byrne, M.; Durbin, A. F.; Hu, X. S.; Iwamoto, N.; Jang, H. G.; et al. Variant-selective stereopure oligonucleotides protect against pathologies associated with C9orf72-repeat expansion in preclinical models. *Nat. Commun.* 2021, 12, No. 847.

(26) Buntz, A.; Killian, T.; Schmid, D.; Seul, H.; Brinkmann, U.; Ravn, J.; Lindholm, M.; Knoetgen, H.; Haucke, V.; Mundigl, O. Quantitative fluorescence imaging determines the absolute number of locked nucleic acid oligonucleotides needed for suppression of target gene expression. *Nucleic Acids Res.* 2019, 47, 953−969.

(27) Pendergraff, H.; Schmidt, S.; Vikeså, J.; Weile, C.; Øverup, C.; Lindholm, M. W.; Koch, T. Nuclear and Cytoplasmatic Quantification of Unconjugated, Label-Free Locked Nucleic Acid Oligonucleotides. *Nucleic Acid Ther.* 2020, 30, 4−13.

(28) Deprey, K.; Becker, L.; Kritzer, J.; Plückthun, A. Trapped! A Critical Evaluation of Methods for Measuring Total Cellular Uptake versus Cytosolic Localization. *Bioconjugate Chem.* 2019, 30, 1006−1027.

(29) Wan, W. B.; Seth, P. P. The Medicinal Chemistry of Therapeutic Oligonucleotides. *J. Med. Chem.* 2016, 59, 9645−9667.

(30) Huang, Z.; Wang, D.; Long, C.-Y.; Li, S.-H.; Wang, X.-Q.; Tan, W. Regulating the Anticancer Efficacy of Sgc8−Combretastatin A4 Conjugates: A Case of Recognizing the Significance of Linker Chemistry for the Design of Aptamer-Based Targeted Drug Delivery Strategies. *J. Am. Chem. Soc* 2021, 143, 8559−8564.

(31) Marcus-Sekura, C.; Woerner, A. M.; Shinozuka, K.; Zon, G.; Quinnan, G. V. Comparative inhibition of chloramphenicol acetyltransferase gene expression by antisense oligonucleotide analogues having alkyl phosphotriester, methylphosphonate and phosphorothioate linkages. *Nucleic Acids Res.* 1987, 15, 5749−5763.

(32) Zhao, Q.; Matson, S.; Herrera, C. J.; Fisher, E.; Yu, H.; Krieg, A. M. Comparison of cellular binding and uptake of antisense phosphodiester, phosphorothioate, and mixed phosphorothioate and methylphosphonate oligonucleotides. *Antisense Res. Dev.* 1993, 3, 53−66.

(33) Beltinger, C.; Saragovi, H. U.; Smith, R. M.; LeSauteur, L.; Shah, N.; DeDionisio, L.; Christensen, L.; Raible, A.; Jarett, L.; Gewirtz, A. M. Binding, uptake, and intracellular trafficking of phosphorothioate-modified oligodeoxynucleotides. *J. Clin. Invest.* 1995, 95, 1814−1823.

(34) Ly, S.; Echeverria, D.; Sousa, J.; Khvorova, A. Single-Stranded Phosphorothioated Regions Enhance Cellular Uptake of Cholesterol-Conjugated siRNA but Not Silencing Efficacy. *Mol. Ther.-Nucleic Acids* 2020, 21, 991−1005.

(35) Wang, S.; Allen, N.; Prakash, T. P.; Liang, X.; Crooke, S. T. Lipid Conjugates Enhance Endosomal Release of Antisense Oligonucleotides Into Cells. *Nucleic Acid Ther.* 2019, 29, 245−255.

(36) Pei, Y.; Hancock, P. J.; Zhang, H.; Bartz, R.; Cherrin, C.; Innocent, N.; Pomerantz, C. J.; Seitzer, J.; Koser, M. L.; Abrams, M. T.; et al. Quantitative evaluation of siRNA delivery in vivo. *RNA* 2010, 16, 2553−2563.